AFRL-RX-WP-TP-2009-4050

QUASISTATIC AND DYNAMIC GROWTH OF MICROSCALE SPHERICAL VOIDS (Preprint)

T.C. Tszeng

Berkeley Materials Research

JANUARY 2008
Interim Report

AIR FORCE RESEARCH LABORATORY
MATERIALS AND MANUFACTURING DIRECTORATE
WRIGHT-PATTERSON AIR FORCE BASE, OH 45433-7750
AIR FORCE MATERIEL COMMAND
UNITED STATES AIR FORCE

REPORT DOCUMENTATION PAGE

Form Approved
OMB No. 0704-0188

1. REPORT DATE *(DD-MM-YY)*	2. REPORT TYPE	3. DATES COVERED *(From - To)*
January 2008	Journal Article Preprint	01 January 2008 – 01 January 2008

4. TITLE AND SUBTITLE
QUASISTATIC AND DYNAMIC GROWTH OF MICROSCALE SPHERICAL VOIDS (Preprint)

5a. CONTRACT NUMBER
FA8650-07-M-5232

5b. GRANT NUMBER

5c. PROGRAM ELEMENT NUMBER
62102F

6. AUTHOR(S)
T.C. Tszeng

5d. PROJECT NUMBER
3005

5e. TASK NUMBER
ML

5f. WORK UNIT NUMBER
222S0400

7. PERFORMING ORGANIZATION NAME(S) AND ADDRESS(ES)
Berkeley Materials Research
431 Linda Ave.
Piedmont CA 94611-4439

8. PERFORMING ORGANIZATION REPORT NUMBER

9. SPONSORING/MONITORING AGENCY NAME(S) AND ADDRESS(ES)
Air Force Research Laboratory
Materials and Manufacturing Directorate
Wright-Patterson Air Force Base, OH 45433-7750
Air Force Materiel Command
United States Air Force

10. SPONSORING/MONITORING AGENCY ACRONYM(S)
AFRL/RXLMN

11. SPONSORING/MONITORING AGENCY REPORT NUMBER(S)
AFRL-RX-WP-TR-2009-4050

12. DISTRIBUTION/AVAILABILITY STATEMENT
Approved for public release; distribution unlimited.

13. SUPPLEMENTARY NOTES
PAO case number WPAFB 08-0101; date cleared: 17 January 2008.

14. ABSTRACT
This study examines the quasistatic and dynamic growth of microscale spherical voids. A general dynamic model of void growth is first developed by considering conservation of local energy, including external work, surface energy, kinetic energy, elastic strain energy, and plastic dissipation associated with growing void driven by hydrostatic tensile stress. It properly accounts for material compressibility and limited size of elastic deformation in dynamic growth of spherical voids. A closed form of pressure-void size relation is obtained for quasistatic growth of spherical voids embedded in non-strain hardening materials. Critical condition is identified for unbounded growth, which depends strongly on initial void size. For subcritical loading, a void can only grow to a very limited size. An interesting crossover phenomenon is identified pertaining to the influences of yield stress on void growth rate.

15. SUBJECT TERMS
Voids, Quasistatic Growth, Dynamic Growth, Microscale

16. SECURITY CLASSIFICATION OF:			17. LIMITATION OF ABSTRACT:	18. NUMBER OF PAGES	19a. NAME OF RESPONSIBLE PERSON (Monitor)
a. REPORT	b. ABSTRACT	c. THIS PAGE			Patrick J. Golden
Unclassified	Unclassified	Unclassified	SAR	46	19b. TELEPHONE NUMBER *(Include Area Code)* (937) 255-6156

Standard Form 298 (Rev. 8-98)
Prescribed by ANSI Std. Z39-18

Quasistatic and Dynamic Growth of Microscale Spherical Voids

T. C. Tszeng

Berkeley Materials Research

Berkeley, CA 94704, USA

Abstract

This study examines the quasistatic and dynamic growth of microscale spherical voids. A general dynamic model of void growth is first developed by considering conservation of local energy, including external work, surface energy, kinetic energy, elastic strain energy, and plastic dissipation associated with growing void driven by hydrostatic tensile stress. It properly accounts for material compressibility and limited size of elastic deformation in dynamic growth of spherical voids. A closed form of pressure-void size relation is obtained for quasistatic growth of spherical voids embedded in non-strain hardening materials. Critical condition is identified for unbounded growth, which depends strongly on initial void size. For subcritical loading, a void can only grow to a very limited size. An interesting crossover phenomenon is identified pertaining to the influences of yield stress on void growth rate.

1. Introduction

The phenomena of nucleation, growth and coalescence of voids are the fundamental mechanism in ductile fracture. Void nucleation can occur through decohesion between a ductile matrix and second-phase particles (Needleman, 1987), or fracture of brittle particles in a ductile matrix. There are indications that lattice defects in the length scale of nanometer can also be the embryo of void nucleation (Lubarda et al., 2004). Once voids have been nucleated, they grow through localized plastic deformation. There are two broad subjects pertaining to void growth: threshold condition and dynamics of void growth. On the first subject, many are also focused on bifurcation and instability. Needleman (1972) established a model to describe the growth of spherical void in elastic-plastic medium. Chung et al. (1987) investigated cavitation bifurcation under a remote hydrostatic tensile loading, and concluded that cavitation pressure was of the order

of Young's modulus. Huang, Hutchinson, and Needleman (1991) addressed quasistatic cavitation instabilities in elastic–plastic materials subjected to multiaxial axisymmetric stressing and found that the condition for unstable void growth depends on the attainment of a critical value of the mean stress. Tvergaard and Hutchinson (1993) extended this analysis to a power hardening elastic–plastic material and also concluded that the occurrence of cavitation instability depends primarily on the level of the mean stress. Hou et al. (1999) considered effects of surface energy on quasistatic growth of spherical and cylindrical voids. Tvergaard and Hutchinson (2002) found that initial void shape had little effect on the critical stress. Thus it appears that both deviations from the hydrostatic state and deviations from the spherical initial void can be neglected in the study of void growth (Wu et al., 2003).

Hunter and Crozier (1968) and Crozier and Hunter (1970) addressed the dynamics of void growth by considering compressibility in elastic-plastic material, and obtained similarity solution for steady-state growth. Most published studies on the dynamics of void expansion take advantage of material incompressibility, and primarily on spherical voids. Rice and Tracey (1969) employed Rayleigh-Ritz approximation to a variational principle for the flow field in an elastically rigid and incompressible plastic material containing a void, subjected to a remotely uniform stress and strain rate field. For spherical voids, Carroll and Holt (1972) addressed the dynamic collapse of a void in an ideally plastic material by using a hollow sphere model. Johnson (1981) extended this approach to rate-dependent materials under hydrostatic tensile loading. The dynamic void collapse and void growth in single crystals under uniform farfield stresses were studied analytically by Nemat-Nasser and Hori (1987). Ortiz and Molinari (1992) considered the dynamic growth of a single void in a power-law hardening material from an energetic viewpoint. Cortes (1992a) extended the spherical shell approach to examine void growth under combined hydrostatic and deviatoric stresses in rigid plastic materials; Cortes (1992b) addressed strain hardening, rate sensitivity and thermal effects of the Johnson–Cook type, but elasticity was neglected because of the assumption that plasticity would quickly dominate the volume. Wang (1994) further extended this approach to model void growth in rate-dependent materials. Wu, Ramesh and Wright (2003) included the influence of thermal diffusion and thermal softening.

There are also studies based on micromechanics of dislocations pertaining to stability and dynamics of void growth (e.g., Stevens et al., 1972; Kameda, 1989; Lubarda et al., 2004; Ohashi, 2005; Ahn et al., 2006, 2007). These studies are mostly focused on high rate, high magnitude loading (e.g., shock) in which deformation mechanisms associated with void formation maybe different from regular loading at low rate. Based upon dislocation micromechanics, the present author has studied the threshold condition in general macroscopic stress state (Tszeng, 2007a), and dynamic model of transient growth (Tszeng 2007b) associated with cylindrical voids. Significant progress has also been achieved recently on void nucleation, growth and coalescence by the technique of atomistic and Molecular Dynamics simulations (e.g., Rudd and Belak, 2002; Seppala et al, 2005).

The subject of dynamic expansion of cylindrical void has been mostly avoided in the past. By assuming incompressibility, it can be shown that total kinetic energy for an expanding spherical void is $K = 2\pi\rho R^3 v^2$ (Ortiz and Molinari, 1992; Wu et al., 2003), where R is void radius and $v = dR/dt$ is the growth rate. If the same procedure is applied to cylindrical void, the kinetic energy would be $K = \pi\rho R^2 v^2 \ln\frac{R_\infty}{R}$, where R_∞ is the outer radius of deformation zone (Tszeng, 2007c). Incompressibility requires $R_\infty \to \infty$ and therefore kinetic energy K is infinite. In another way, stress equilibrium in radial direction of a cylindrical void can be written as (Crozier and Hunter, 1970; Tszeng, 2007c, d):

$$\frac{\partial \sigma_r}{\partial r} - \frac{\bar{\sigma}}{r} = \rho \frac{R\frac{d^2R}{dt^2} + \frac{dR}{dt}}{r}, \qquad (1)$$

where σ_r is radial stress, R_o initial void radius, G shear modulus, and ρ mass density. Logarithmic singularity results from integrating the terms on the right-hand side of Eq. (1) to infinity. Its implication is a zero growth rate for cylindrical void. Obviously, infinite deformation zone is the underlining issue that prevents the nonsingular solution. Therefore, Crozier and Hunter (1970) and Warren (1999) declared that no physically realistic solution is possible for steady dynamic expansion of long cylindrical cavities (plane-strain assumption) in an incompressible

elastoplastic medium, due to logarithmic stress divergence in the remote elastic field. Warren (1999) examined the effects of strain rate on the model of Crozier and Hunter (1970) for cylindrical void in steady expansion. Just recently, Masri and Durban (2006) challenged the declaration of Crozier and Hunter (1970), and obtained self-similar solutions to the model of steady-state growth using hypoelasticity J_2 theory. A disposable constant was used to remove stress singularity. Unfortunately, as pointed out in Tszeng (2007c), there is a severe internal inconsistency that defeats the validity of that model. That is, stress singularity does exist, and the solution is approximate, at the best. In the case of spherical void, stress equilibrium in radial direction is (Wu et al, 2003)

$$\frac{\partial \sigma_r}{\partial r} - \frac{2\bar{\sigma}}{r} = \rho\left(\frac{R\ddot{R} + 2R\dot{R}^2}{r^2} - 2\frac{R^4\dot{R}^2}{r^5}\right), \tag{2}$$

Integrating the terms on the right-hand side of Eq. (2) to infinity does not lead to singularity. The nonsingular solution is, however, an approximation valid for incompressible materials. It is believed that considerations should be given to limited deformation zone to circumvent the same issue that prevents proper description of the dynamics of expanding cylindrical voids.

This paper examines the quasistatic and dynamic growth of spherical voids in sub-micron length scales. A general dynamic model of void growth is first developed by considering conservation of local energy, including external work, surface energy, kinetic energy, elastic strain energy, and plastic dissipation associated with growing void driven by hydrostatic tensile stress. Special attention is placed on the development of a proper expression of kinetic energy in the material surrounding an expanding void. In Section 2, the governing equation of void growth is established. Section 3 examines quasistatic growth and threshold conditions. Lastly, dynamic growth is discussed in Section 4, with special emphasis on steady-state growth.

2. Dynamic Model of Void Growth

A common difficulty to most dynamic models of void growth in the past stems from the fact that deformation extends to infinity for incompressible material. Recognizing this fact, Hunter and Crozier (1968) considered compressibility in material surrounding an expanding void. They

obtained similarity solutions to the problem of steady growth of spherical voids. Obviously, the solutions are limited in applicability.

The present approach considers a system that contains a single spherical void embedded in an infinite elastic-plastic matrix. The space is divided into several zones, including void itself, incompressible plastic zone, compressible elastic zone, and undisturbed material (Fig. 1). In the following, equations are formulated for elastic and plastic zones in the framework of continuum. Solutions are sought for plastic and elastic zones, respectively, with proper continuity imposed at the interface. In particular, the radial stress on plastic-elastic interface is determined by the solution of elastic zone. As will be further elaborated in Section 3, solution of radial stress on plastic-elastic interface as obtained by Hunter and Crozier (1968) does not reconcile with the solutions based upon near-incompressible materials or low-rate growth. On the other hand, an approximate solution is obtained, which is applicable for general dynamic, transient growth.

2.1 Solution for the plastic zone

A void has radius R at current time t_i; its surface moves outwards at radial velocity v (Fig. 1). Material gains kinetic energy associated with moving void surface. There is energy dissipation due to plastic deformation and surface energy expenditure for expanding void surface. The law of energy conservation states that,

$$\dot{W} = \dot{\Gamma} + \dot{K} + \dot{\Phi}, \tag{3}$$

where $\dot{W}$ is input power done by externally applied stress/strain, $\dot{\Gamma}$ surface energy, $\dot{K}$ kinetic energy, and $\dot{\Phi}$ plastic dissipation. Elastic strain energy is neglected in plastic zone (will be considered in the outer elastic zone; see Sections 2.2. and 2.3). Eq. (3) says that surface energy and kinetic energy increase at the expense of externally supplied energy, with additional energy dissipating in plastic deformation.

The plastically deforming matrix has a radius $D > R$. The incremental displacement at the outer boundary of matrix material at radius D in a time interval dt is du. Assume the radial stress

appears at $r = D$ is σ_D, the work done in plastic zone is $dW = 4\pi D^2 \sigma_D du$. The explicit expression of σ_D is determined in Sections 2.2 and 2.3. By considering incompressibility of material between R and D, radial velocity at $r \in$ (R, D) is (Carroll and Holt, 1972; Ortiz and Molinari, 1992)

$$v_r = (R/r)^2 v, \tag{4}$$

where $v = dR/dt$ is void growth rate. Radial velocity at the outer surface of matrix is $v_D = \frac{R^2}{D^2} v$. Therefore, rate of energy input to the plastic zone is

$$\dot{W} = 4\pi R^2 \sigma_D v. \tag{5}$$

Change of surface energy is written as $d\Gamma = \gamma dS$ where γ is surface energy density. Increase of void surface $dS = 4\pi(R + dR)^2 - 4\pi R^2 = 8\pi R dR$. Hence,

$$\dot{\Gamma} = 8\pi\gamma R v. \tag{6}$$

Material in the vicinity of void surface gains velocity which is in the form of Eq. (4). Kinetic energy corresponding to an incremental mass at radius r is $dK = \frac{1}{2} v_r^2 dm = 2\pi\rho r^2 v_r^2 dr$, where ρ is mass density. Total kinetic energy in plastic zone is

$$K = (\frac{4}{3}\pi\rho R^3)(\frac{v^2}{2})\alpha, \tag{7}$$

where $\alpha = 3(1 - 1/\beta)$, and $\beta = D/R$. In contrast, the counterpart in a cylindrical void is $K = (\pi\rho R^2)(\frac{v^2}{2})\alpha$ where $\alpha = 2\ln\beta$ (Tszeng, 2007c). In both cases, the expression preceding α represents the mass of void. Again, the geometrical factor α defines the influence of size of plastic

zone on the dynamics of void growth. The specific expression of D will be discussed later in this section. Change in kinetic energy between t_i and $t_i + dt$, is

$$dK = \frac{2}{3}\pi\rho\alpha(R+dR)^3(v+dv)^2 - \frac{2}{3}\pi\rho\alpha R^3 v^2 .$$

After removing higher order terms, one obtains the expression of changing rate of kinetic energy:

$$\dot{K} = 2\pi\rho\alpha R^2 v^3 + \frac{4}{3}\pi\rho\alpha R^3 v\frac{dv}{dt} \tag{8}$$

The last term in Eq. (3) is plastic dissipation, $\dot{\Phi}$. Specific plastic dissipation rate, $\dot{W}^P$ (dissipation rate per unit volume), is

$$\dot{W}^P = \bar{\sigma}\dot{\bar{\varepsilon}}, \tag{9}$$

where $\bar{\sigma}$ and $\dot{\bar{\varepsilon}}$ are the effective stress and effective strain rate, respectively. In plastic zone, elastic strain is neglected; and total strain is equal to plastic strain; i.e., $\dot{\bar{\varepsilon}} = \dot{\bar{\varepsilon}}^P$. For simple strain hardening materials,

$$\bar{\sigma} = \sigma_Y f(\bar{\varepsilon}^P) \tag{10}$$

In the present case of spherical deformation (Hou et al., 1999),

$$\bar{\varepsilon} = -\varepsilon_r, \text{ and } \varepsilon_r = -2\varepsilon_\theta = \frac{2}{3}\ln(1 - \frac{R^3 - R_o^3}{r^3}), \tag{11}$$

and

$$\dot{\bar{\varepsilon}}^P = -\dot{\varepsilon}_r^P = 2\frac{v_r}{r} = 2(\frac{R}{r})^2\frac{v}{r}, \tag{12}$$

By Eqs. (9), (10), and (12), specific plastic dissipation rate per unit volume is

$$\dot{W}^P = 2\sigma_Y f(\bar{\varepsilon}^P)(\frac{R}{r})^2 \frac{v}{r}. \tag{13}$$

Total plastic dissipation rate associated with an expanding spherical void can now be written as

$$\dot{\Phi} = \int_V \sigma_Y f(\bar{\varepsilon}^P)(\frac{R}{r})^2 \frac{v}{r} dV = 8\pi R^2 \sigma_Y v \int_R^D f(\bar{\varepsilon}^P)\frac{dr}{r}. \tag{14}$$

Hence, incremental plastic dissipation is found to be

$$\dot{\Phi} = 4\pi R^2 \hat{\sigma}_Y v, \tag{15}$$

where equivalent flow stress, $\hat{\sigma}_Y$, is defined by

$$\hat{\sigma}_Y = 2\sigma_Y \int_R^D f(\bar{\varepsilon}^P)\frac{dr}{r}. \tag{16}$$

Eq. (16) can be further converted in a form found in literature. By using Eq. (11) and some algebraic operations, it can be shown that $\frac{dr}{r} = -\frac{1}{2}\frac{d\bar{\varepsilon}}{\exp(\frac{3}{2}\bar{\varepsilon}) - 1}$. Therefore,

$\hat{\sigma}_Y = -\sigma_Y \int_{\bar{\varepsilon}_1}^{\bar{\varepsilon}_2} \frac{f(\bar{\varepsilon}^P)d\bar{\varepsilon}}{\exp(\frac{3}{2}\bar{\varepsilon}) - 1}$, where $\bar{\varepsilon}_1$ and $\bar{\varepsilon}_2$ are the effective strains at $r = R$ and D, respectively.

By Eq. (11) again, $\bar{\varepsilon}_1 = -2\ln(R_o / R) = 2\ln(R / R_o)$ is the strain on void surface, and

$\bar{\varepsilon}_2 = \varepsilon_Y = \frac{2}{3}\ln(1 - \frac{R^3 - R_o^3}{D^3})$ corresponds to the strain on the boundary of plastic zone. In this expression, ε_Y is the strain at yielding ($\varepsilon_Y = \sigma_Y / E$). After swapping the integration limits, the expression of equivalent flow stress in Eq. (16) becomes,

$$\hat{\sigma}_Y = \sigma_Y \int_{\varepsilon_Y}^{2\ln(R/R_o)} \frac{f(\bar{\varepsilon})d\bar{\varepsilon}}{\exp(\frac{3}{2}\bar{\varepsilon})-1} \tag{17}$$

Eqs. (5), (6), (8), and (15) give the formula of each term involving local energy conservation. Placing them in Eq. (3), one obtains the ordinary differential equation:

$$\frac{1}{3}\rho\alpha R\frac{dv}{dt}+\frac{\rho}{2}\alpha v^2 = \sigma_D - (\hat{\sigma}_Y + \frac{2\gamma}{R}) \tag{18}$$

This is the equation governing dynamic void growth of a single spherical void embedded in infinite matrix. The radial stress on yield surface, σ_D, is yet to be identified in Sections 2.2 and 2.3.

In Eq. (18), the factor α is not determined either. The boundary of plastic zone is defined by the location at which $\bar{\varepsilon} = \varepsilon_Y$. According to Eq. (11), the boundary of plastic zone is located at radius D:

$$\beta = \frac{D}{R} = [1-\exp(-\frac{3}{2}\varepsilon_Y)]^{-1/3}, \text{ for } R >> R_o. \tag{19}$$

By the approximation $1-\exp(-\frac{3}{2}\varepsilon_Y) \approx \frac{3}{2}\varepsilon_Y$, one has the expression (Huang et al., 1991):

$$\beta = (\frac{3}{2}\varepsilon_Y)^{-1/3}, \quad \text{for } R >> R_o. \tag{20a}$$

As a side note, Eq. (20a) is actually valid for incompressible materials; the general expression ought to be (Hill, 1989).

$$\beta = [3(1-\nu)\varepsilon_Y]^{-1/3}. \tag{20b}$$

This ratio is presumably a material constant. Hence,

$$\alpha = 3[1-(3(1-\nu)\varepsilon_Y)^{1/3}] \tag{21}$$

The equivalent flow stress $\hat{\sigma}_Y$ of Eq. (17) is usually integrated numerically providing the function f is specified. In case a time-stepping method is used for calculating the progress of void size, $\hat{\sigma}_Y$ needs to be updated accordingly for each time step. As will be shown later, radial stress, σ_D, is also dependent upon current solution, and needs to be updated.

2.2 Solution for the elastic zone – Steady state

The objective of this section is to determine the radial stress, σ_D, on yield surface at $r = D$ in steady state growth. The solution was obtained previously by Hunter and Crozier (1968). We furnish the following formulation with additional purpose of laying the ground for developing a competing model to be used for general, transient void growth (Section 2.3). The solution is first sought for the problem corresponding to a boundary problem in which constant velocity is specified on the inner boundary of elastic zone. Superposition principle is then employed to determine the radial stress, σ_D. Identical results are obtained in an alternative approach by solving the complete equilibrium equation (Tszeng, 2007d).

The outer boundary of elastic zone is determined by the travel distance of dilatational elastic wave whose speed is

$$c_e = (\frac{\lambda + 2G}{\rho})^{\frac{1}{2}}, \tag{22}$$

where λ is Lame elastic constant, G shear modulus, and ρ mass density. It is assumed that void grows from a negligibly small size. At time t, the location of outer boundary is given by $C = c_e t$; elastic zone is defined between D and C (Fig. 1). Similarity solution of particle displacement, u, in the compressible elastic zone is obtained by Hunter and Crozier (1968) for steady-state growth:

$$u = At(\frac{2}{3}\eta - 1 + \frac{1}{3}\eta^{-2}), \tag{23}$$

where the dimensionless similarity variable $\eta = \frac{r}{c_e t}$, and A is a coefficient independent of η.

Particle velocity at a location r $\in$ (D, C) in elastic zone is $v_r = du/dt$. By using Eq. (23), it can be shown that velocity in elastic zone is:

$$v_r = A(-1+\eta^{-2}) = A\frac{(c_e t)^2 - r^2}{r^2}, \tag{24}$$

Unlike Hunter and Crozier (1968), the present study assumes an incompressible plastic zone.

Particle velocity at the interface of elastic and plastic zone ($r = D$) is $v_D = \frac{R^2}{D^2}v$. The coefficient A can then be determined by imposing velocity continuity at elastic-plastic interface; the result is

$$A = v\frac{\eta_R^2}{1-\beta^2\eta_R^2}. \tag{25}$$

where $\eta_R = \frac{R}{c_e t}$.Therefore, velocity field in elastic zone is

$$v_r = \frac{1-\eta^2}{1-\beta^2\eta_R^2}\frac{R^2}{r^2}v. \tag{26}$$

On yield surface, von Mises yield criterion is

$$\sigma_\theta - \sigma_r = \sigma_Y. \tag{27}$$

By Hooke's law,

$$\sigma_\theta = \frac{E}{1-\nu}\left(\frac{\nu}{E}\sigma_r + \varepsilon_\theta\right) = \frac{\nu}{1-\nu}\sigma_r + \frac{u}{D}. \tag{28}$$

Replace Eq. (28) in Eq. (27), the radial stress is σ_r written as

$$\sigma_r = \frac{E}{1-2\nu}\frac{u}{D} - \frac{1-\nu}{1-2\nu}\sigma_Y. \tag{29}$$

By Eq. (23) in conjunction with Eq. (25), it can be shown that

$$\frac{u}{D} = \frac{1+\nu}{3E}\sigma_Y\left[1 - \frac{2}{1+\beta\eta_R}(\beta\eta_R)^2\right]. \tag{30}$$

By combining Eqs. (29) and (30), the radial stress induced by a specified velocity on the inner boundary of elastic zone is

$$\sigma_r = -\frac{2}{3}\sigma_Y\left(1 + \frac{1+\nu}{1-2\nu}\frac{\beta^2\eta_R^2}{1+\beta\eta_R}\right), \tag{31}$$

It can be shown that radial stress of Eq. (31) is identical to that of Hunter and Crozier (1968) in steady-state growth. For a material subjected to macroscopic hydrostatic stress P, the solution can be obtained by simple superposition; i.e., $\sigma_D = P + \sigma_r$. Therefore, the radial stress on yield surface,

$$\sigma_D = P - \frac{2}{3}\sigma_Y - \frac{2}{3}\sigma_Y\frac{1+\nu}{1-2\nu}\frac{\beta^2\eta_R^2}{1+\beta\eta_R}, \tag{32}$$

The expression of Eq. (32) can also be derived by solving the stress equilibrium in radial direction, as shown in a separate paper (Tszeng, 2007d).

By using Eqs. (20b) and (22), Eq. (32) is further reduced to

$$\sigma_D = P - \frac{2}{3}\sigma_Y - \frac{\rho}{2}\omega v^2 \tag{33}$$

where

$$\omega = \frac{1}{\beta(1+\beta\bar{v})}\frac{4}{9}\left(\frac{1+\nu}{1-\nu}\right)^2. \tag{34}$$

The radial stress on yield surface, σ_D, of Eq. (33) is to be used in the governing equation of Eq. (18) for steady-state growth. The solution represented by Eq. (33) is exact, subjected to the assumptions herein (Hunter and Crozier, 1968). However, as will be further elaborated in Section 3, it does not reconcile with the solutions based upon incompressible materials.

2.3 Solution for the elastic zone – Transient

The solution presented in Section 2.2 is valid for steady-state growth. A competing but less exact solution is now developed for general dynamic, transient growth. In the present formulation, plastic zone adjacent to elastic zone is assumed incompressible. Once the macroscopic stress exceeds a threshold condition, plastic zone is established immediately. Compressibility in elastic zone is considered in addressing the kinetic energy only; otherwise incompressibility is still assumed in calculating elastic strain energy. The rationale is that dynamics of an expanding void have the greatest influence on kinetic energy, and less on elastic strain energy.

The formulation is in analogy to that of Section 2.1. Local energy conservation is in a form similar to that of Eq. (2)

$$\dot{W} = \dot{K} + \dot{\Psi}, \tag{35}$$

where $\dot{W}$ is input power done by externally applied stress/strain, $\dot{K}$ kinetic energy, and $\dot{\Psi}$ strain energy. Each term is formulated in the following. Total energy input to elastic zone is

$$\dot{W} = 4\pi R^2 (P - \sigma_D) v \tag{36}$$

Total kinetic energy in elastic zone is $K = \int 2\pi\rho r^2 v_r^2 dr$. Velocity field in elastic zone is given by Eq. (26) for steady-state growth. Nonetheless, this equation describes a permissible velocity that satisfies boundary conditions. As an approximation, we use the same expression to describe the snap shot of velocity field in elastic zone at any time *t*; that is,

$$v_r = \frac{(c_e t)^2 - r^2}{(c_e t)^2 - D^2} \frac{R^2}{r^2} v. \tag{37}$$

It is remarked that the velocity *v* needs not to be a constant anymore. It can be proven that the condition of velocity continuity at elastic-plastic boundary also satisfies the yielding condition. Total kinetic energy is obtained for elastic zone between D and $c_e t$. After some algebra operations, the result is

$$K = (\frac{4}{3}\pi\rho R^3)(\frac{v^2}{2})\kappa, \tag{38}$$

where

$$\kappa = \frac{(3+\beta\bar{v})(1-\beta\bar{v})}{\beta(1+\beta\bar{v})^2}, \tag{39}$$

and normalized average growth rate $\bar{v} = \frac{1}{c_e t}\int v dt = \frac{R}{c_e t}$. Actually, $\bar{v} = \eta_R$, but it is more convenient to use $\bar{v}$ for the cases of transient growth being dealt with in this section. Since Eq. (38) is in the same form of Eq. (7), it is easy to show that changing rate in kinetic energy is

$$\dot{K} = 2\pi\rho\kappa R^2 v^3 + \frac{4}{3}\pi\rho\kappa R^3 v\frac{dv}{dt} \tag{40}$$

The last term in Eq. (35) is rate of elastic strain energy, $\dot{\Psi}$. Specific rate of strain energy is in the same form of Eq. (9), except the effective stress for linear elastic response is

$$\overline{\sigma} = \sigma_Y \frac{\overline{\varepsilon}}{\varepsilon_Y}, \quad \text{for } \overline{\varepsilon} \le \varepsilon_Y. \tag{41}$$

Because incompressibility is retained in considering elastic strain energy, strain energy rate follows that of Eqs. (13) and (14). That is

$$\dot{\Psi} = \int_V \sigma_Y f(\overline{\varepsilon}^P)(\frac{R}{r})^2 \frac{v}{r} dV = 8\pi R^2 \sigma_Y v \int_0^{\varepsilon_f} \frac{\overline{\varepsilon}}{\varepsilon_Y}\frac{dr}{r}, \tag{42}$$

Again, incompressibility allows us to write $\frac{dr}{r} = -\frac{1}{2}\frac{d\overline{\varepsilon}}{\exp(\frac{3}{2}\overline{\varepsilon}) - 1}$. Since $\overline{\varepsilon}$ $(\le \varepsilon_Y)$ is a very small number; $\exp(\frac{3}{2}\overline{\varepsilon}) \approx 1 + \frac{3}{2}\overline{\varepsilon}$. Therefore, $\frac{dr}{r} = -\frac{1}{3}\frac{d\overline{\varepsilon}}{\overline{\varepsilon}}$. Replacing this expression in Eq. (42), $\dot{\Psi} = -8\pi R^2 \sigma_Y v \int_{\varepsilon_Y}^{0} \frac{d\overline{\varepsilon}}{3\varepsilon_Y} = \frac{8}{3}\pi R^2 \sigma_Y v$, where the proper integration limits are used. Therefore,

$$\dot{\Psi} = \frac{8}{3}\pi R^2 \sigma_Y v \tag{43}$$

Eqs. (36), (40) and (43) give the formula of each term involving local energy in elastic zone. Placing them in Eq. (35), we obtain the radial stress on yield surface:

$$\sigma_D = P - \frac{2}{3}\sigma_Y - (\frac{1}{3}\rho\kappa R\frac{dv}{dt} + \frac{1}{2}\rho\kappa v^2) \tag{44}$$

Combining Eq. (44) with Eq. (18), we obtain the governing equation for dynamic, transient void growth. The development of a dynamic model of spherical void growth is thus completed.

3. Threshold condition and quasistatic void growth

We first examine the situations that dynamics effects are negligible. Many prior studies have been devoted to examine this subject, see review in Section 1. Among others, quasistatic growth of spherical void has been studied by Huo et al (1999) who considered surface energy. Wu et al (2003) also worked on the model with materials possessing various strain and strain-rate sensitivity. However, that work does not consider the effects of surface energy. The example calculations presented in the following only involve non-straining materials; applications of the developed model to more general material behaviors will be reported elsewhere.

By Eqs. (33) or (44), we recognize that radial stress on yielding surface in quasistatic growth is

$$\sigma_D = P - \frac{2}{3}\sigma_Y \tag{45}$$

Eq. (18) is then simplified to the following equation if dynamic effects are dropped altogether:

$$P = \frac{2}{3}\sigma_Y + \frac{2}{R}\gamma + \sigma_Y \int_{\varepsilon_Y}^{2\ln(R/R_o)} \frac{f(\bar{\varepsilon})d\bar{\varepsilon}}{\exp(\frac{3}{2}\bar{\varepsilon}) - 1} \tag{46}$$

Eq. (46) is in the same form as that of Huo et al (1999) except the lower limit of integration is ε_Y instead of zero in Hou et al (1999). The lower limit of ε_Y is the strain at boundary of plastic zone ($r = D$). Integration of Eq. (46) is carried out for non-strain hardening materials; i.e., $f(\bar{\varepsilon}) = 1$. By changing variables, the analytical form of integration is:

$$\int \frac{d\bar{\varepsilon}}{\exp(\frac{3}{2}\bar{\varepsilon})-1} = \frac{2}{3}\ln[1-\exp(-\frac{3}{2}\bar{\varepsilon})]. \qquad (47)$$

By integrating between aforementioned limits, we obtain the relation between applied pressure, P, and void size, R:

$$P = \frac{2\gamma}{R} + \frac{2}{3}\sigma_Y + \frac{2}{3}\sigma_Y \ln\frac{1-\frac{R_o^3}{R^3}}{1-\exp(-\frac{3}{2}\varepsilon_Y)}. \qquad (48)$$

It is surprising that, after many papers published in literature, the closed form of Eq. (48) is obtained for the first time. By approximating $1-\exp(-\frac{3}{2}\varepsilon_Y) \approx \frac{3}{2}\varepsilon_Y$,

$$\frac{P}{\sigma_Y} = \frac{2}{R}\frac{\gamma}{\sigma_Y} + \frac{2}{3} + \frac{2}{3}\ln[(1-\frac{R_o^3}{R^3})\frac{2}{3\varepsilon_Y}]. \qquad (49)$$

Obviously, the denominator becomes zero if lower limit of integration, ε_Y, is zero. Thus, the model of Huo et al. (1999) breaks down for single void embedded in infinite matrix (at zero void fraction, $V_f = 0$).

We first consider a hypothetical case in which surface energy can be ignored ($\gamma = 0$). For instance, systems with large isolated voids fall into this category. Since the logarithmic term on the RHS of Eq. (49) represents energy dissipation, it cannot be negative. At initial yielding, zero dissipation implies $\ln[(1-\frac{R_o^3}{R^3})\frac{2}{3\varepsilon_Y}] = 0$; and the corresponding macroscopic stress by Eq. (49) is $P = 2\sigma_Y/3$. That is, void starts expansion by yielding on void surface at $P = 2\sigma_Y/3$. The same conclusion can also be obtained by examining Eq. (45). On void surface where initial yielding starts, the radial stress is zero, $\sigma_r = \sigma_D = 0$. By Eq. (45), the corresponding macroscopic stress is

$P = 2\sigma_Y / 3$. At the minimum macroscopic stress of $P = 2\sigma_Y / 3$ for initial yielding, the condition of $\ln[(1-\frac{R_o^3}{R^3})\frac{2}{3\varepsilon_Y}] = 0$ gives the new void size upon initial yielding as,

$$\frac{R}{R_o} = (1-\frac{3\varepsilon_Y}{2})^{-1/3} \approx 1+\frac{\varepsilon_Y}{2} \tag{50}$$

At a typical value of $\varepsilon_Y = 0.002$, the growth of void size is about 0.1%. Although 0.1% is a small expansion, repeated loading can raise the size indefinitely. For example, 1,000 cycles of loading at minimum stress of $P = 2\sigma_Y / 3$ result in 100% void expansion. On the other hand, at this absolute minimum loading, the growth rate is zero ($v = 0$) and void does not grow at all in theory. At a loading below the minimum stress, no plastic yielding ever takes place, and the system remains entirely elastic.

For the hypothetical case of zero surface energy, Fig. 2 shows the calculated results of P/σ_Y versus normalized void radius, R/R_o, according to Eq. (49) for a range of yield plastic strain ε_Y. The results in Fig. 2 are supposed to be identical to that of Huang et al. (1991). As shown, equilibrium void size increases very rapidly as the applied pressure approaching an asymptotic value. Equilibrium void size does not exist for stress exceeding a so-called threshold stress, P_∞ (e.g., Huang et al., 1991; Wu et al., 2003). The threshold stress is obtained by letting $R \to \infty$ in Eq. (49); i.e.,

$$P_\infty = P|_{R\to\infty} = \frac{2}{3}(1+\ln\frac{2}{3\varepsilon_Y})\sigma_Y . \tag{51}$$

The threshold stress of Eq. (51) is identical to that of Huang et al. (1991) and others. Therefore, for a loading $P < P_\infty$, void grows to a finite, equilibrium size determined by Eq. (49) (shown in Fig. 2). Once loading exceeds the threshold stress P_∞, void can grow indefinitely with growth rate determined by the inertial associated with dynamic growth (see Section 4).

With zero surface energy ($\gamma = 0$) in Eq. (49), the conditions $R \to \infty$ and $R_o \to 0$ lead to the same results of Eq. (51). The latter is called cavitation limit (e.g., Huang et al., 1991). However, in light of the complete formulation of Eq. (49) with effects of surface energy, the conditions $R \to \infty$ and $R_o \to 0$ are not the same. In the latter case, surface energy term, $\frac{2}{R}\frac{\gamma}{\sigma_Y}$, becomes infinity for void to grow from $R_o \to 0$. It is not possible for cavitation to take place from a mathematical point of zero size. This conclusion is quite different from previous studies in this respect.

Void growth with effects of surface energy is shown in Fig. 3. For comparison purposes, material data of Huo et al (1999) are used here; i.e., $\gamma = 1$ J/m^2, $\sigma_Y = 200$ MPa, $E = 130$ GPa, and mass density $\rho = 8{,}950$ Kg/m^3. Since surface energy is significant only for very small voids, initial void radius, R_o, as small as 2 nm are shown in the figure (although the applicability of continuum approach becomes highly questionable at this small length scale). Overall, surface energy adds additional requirement on applied stress to expand voids. As void grows much bigger, the term involving surface energy, $\frac{2}{R}\frac{\gamma}{\sigma_Y}$, in Eq. (49) diminishes; the ratio P/σ_Y approaches the asymptotic value of Eq. (51).

Unlike the cases with $\gamma = 0$ which is monotonic, an interesting characteristic in the curves of P/σ_Y versus R/R_o in Fig. 3 is the existence of peaks. For example, for $R_o = 5nm$, P/σ_Y reaches the peak value of 5.838 at $R/R_o = 1.328$, although it takes lower stress P for the void to continue growing once void size pass the peak. Therefore, if the applied stress exceeds the peak stress of $P/\sigma_Y = 5.838$, void becomes unstable and expansion continues indefinitely. We will call this as the *critical stress,* σ_c, for unbounded void growth. The existence of critical stress is not unexpected. Void growing from small initial size needs to overcome the resistance due to surface energy (surface tension), which decreases with large void size. On the other hand, resistance due to elastic-plastic deformation increases with void size. Therefore, there is a transitional void size at which applied stress is balanced by surface energy and plastic deformation. At that critical

condition, void does not grow. The critical condition is corresponding to $dP/dR = 0$, where P is given by Eq. (49). It can be shown that the critical condition leads to the following equation:

$$\frac{\sigma_Y}{\gamma} R_c = (\frac{R_c}{R_o})^3 - 1.$$

where R_c is void size at critical condition. Once the critical void size, R_c, is obtained, the corresponding critical stress, σ_c, is calculated by Eq. (49). The above equation is solved numerically; and results are shown in Fig. 4 for a range of initial void radius, R_o. The influence of specific surface energy γ is also shown. For the void of initial size $R_o = 5nm$ embedded in model material with $\sigma_Y = 200$ MPa, the critical stress is 1.16 GPa ($5.838\sigma_Y$) for $\gamma = 1$, and 1.47 GPa ($7.349\sigma_Y$) for $\gamma = 2$. Loading at the cavitation limit stress of Eq. (51) does not lead to cavitation at all, due to the rapidly increasing surface energy term $\frac{2}{R}\frac{\gamma}{\sigma_Y}$. It does not lead to unbounded growth from a small initial void either. For a void to grow indefinitely, the applied stress needs to overcome the aforementioned critical stress, σ_c. It is also noted that the critical stresses corresponding to different initial void sizes eventually converge to a single asymptotic value at large void size, which is the threshold stress of Eq. (51).

With the effects of surface energy being considered, initial yielding takes place at a stress higher than $P = 2\sigma_Y/3$ quoted earlier. According to Eq. (49), the minimum stress for initial yielding would be

$$P = \frac{2}{R}\gamma + \frac{2}{3}\sigma_Y. \qquad (52)$$

Again, the same expression of Eq. (52) can be obtained by examining Eq. (45). On void surface where initial yielding takes place, surface energy leads to a surface normal traction of $T = \frac{2\gamma}{R}$, pointing toward void center (Gent and Tompkins, 1969). That is, the radial stress on void surface is

$\sigma_r = \sigma_D = 2\gamma / R$. By Eq. (45), the corresponding loading is $P = 2\gamma / R + 2\sigma_Y / 3$. This expression is identical to Eq. (52). The dependency of macroscopic stress for initial yielding on void size is calculated, and shown in Fig. 4 using data of model material. Obviously, the effects of surface energy are dominant for the range of void size considered in the figure. For void of radius R = 30 nm, contributions of surface energy and yield stress to the loading for initial yielding are equal (for the model material); at larger void size, the role of surface energy becomes less significant.

4. Dynamic void growth

Dynamic void growth has been the subject of a number of papers, including Carroll (1972), Cortes et al (1992, 1995), Ortiz and Molinari (1992), Wu et al. (2003). The present model, as represented by Eq. (18) in conjunction with Eq. (33) or (44), however, contains correction factor α to account for the limited plastic zone surrounding a growing void; and κ for compressible elastic zone. In light of these improvements, the results are expected to be more accurate than those in existing literatures. Again, this study only examines non-strain hardening materials; more general applications of the developed model will be reported elsewhere. The considered loading is a constant hydrostatic stress that is applied instantly at time zero. This type of loading prevents the additional effects of loading speed like that considered in Wu et al. (2003). In the following, steady-state growth will be examined first, followed by a brief discussion and example calculations of transient growth.

4.1 Steady-state growth

In steady state growth, $dR/dt = v$ = constant. The two approaches of Sections 2.2 and 2.3 lead to different forms of radial stress on yield surface, σ_D in Eq. (33) and (44), respectively. Before engaging a full-flange comparison between Eqs. (33) and (44), it will prove rewarding to examine the asymptotic condition of void growth at very low rate ($v \to 0$) or in materials with near-incompressibility ($c_e \to \infty$). In either case, we have the condition of $\bar{v} = v / c_e \to 0$. Replacing σ_D from Eq. (33) into Eq. (18) for steady state growth, and assuming $R >> R_o$,

$$\frac{\rho}{2}(\alpha+\omega)v^2 = P - P_\infty, \tag{53}$$

where threshold stress P_∞ is given by Eq. (51). It can be shown by using Eq. (34) that $\omega \to \frac{1}{\beta}\frac{4}{9}(\frac{1+\nu}{1-\nu})^2$ as $\bar{v} \to 0$. For near-incompressible materials ($\nu \to 1/2$), $\omega \to 4/\beta$. On the other hand, replacing σ_D from Eq. (44) into Eq. (18) for steady state growth:

$$\frac{\rho}{2}(\alpha+\kappa)v^2 = P - P_\infty \tag{54}$$

By using Eq. (39), it is easy to show that $\kappa \to 3/\beta$ as $\bar{v} \to 0$. For incompressible materials, the coefficient in parentheses on the LHS of Eq. (53) is $\sigma + \frac{4}{\beta}$ in contrast to $\alpha + \frac{3}{\beta}$ in Eq. (54). Accordingly, the model of Hunter and Crozier (1968) gives lower steady-state growth rate in near-incompressible materials than that predicted by the model of Eq. (54).

For near-incompressible materials, deformation (elastic) zone extends to infinity in the same way as has been addressed in the literatures. By integrating the terms on the RHS of Eq. (2) from R to infinity, the result is $\frac{3\rho}{2}v^2$. Actually, the governing equation for near-incompressible materials should have been written as:

$$\frac{3\rho}{2}v^2 = P - P_\infty. \tag{55}$$

This is the conventional model (e.g., Wu et al., 2003, with added surface energy term), assuming incompressibility for material surrounding an expanding void. If one replaces the relation of $\alpha = 3(1-1/\beta)$ on the LHS of Eq. (54), the equation is then identical to Eq. (55). That is, the model of Section 2.3 reconciles with the existing dynamic model for steady-state void growth in near-incompressible materials. Conversely, the model of Hunter and Crozier (1968) fails to do the same.

To further compare the two approaches of Sections 2.2 (i.e., Eq. 33) and 2.3 (i.e., Eq. 44), we are focused on the terms ω in Eq. (34) against κ in Eq. (39). The calculated results of these terms ($\beta\kappa$ and $\beta\omega$) are shown in Fig. 5(a) for two values of Poisson's ratio (0.25 and 0.499999) over a range of growth rate v. The normalized growth rate $\bar{v} = 0.144$ for $v = 600$ m/s based on a Poisson's ratio $\nu = 0.25$. As growth rate v approaching zero, the value of $\beta\kappa$ approaches to 3, regardless of the value of Poisson's ratio, ν. The value of $\beta\omega$ does not converge at all. Since the value of $\beta\kappa$ deviates from 3 at higher growth rate v, the difference increases between the present model represented by Eq. (54) and the conventional model of Eq. (55).

Fig. 5(b) shows the calculated normalized pressure, $(P-P_\infty)/\rho c_e^2$, versus growth rate, v. Material data are taken from the model material except the indicated Poisson's ratio. In Fig. 5(b), the curve of $\nu \to 0.5$ by using the present model of Section 2.3 (labeled Tszeng) is identical to the conventional model; i.e., Eq. (55). Incompressible material requires higher pressure to reach the same growth rate; due to larger elastic deformation zone (actually infinity). Although the results of Tszeng differ only slightly from that of Hunter-Crozier, the former is considered more favorable. The seemly big discrepancy between κ and ω in Fig. 5(a) does not translate to significant difference in calculated pressure shown in Fig. 5(b). The reason is that the factor α is much larger than κ in Eq. (54) or ω in Eq. (53); changes in factors κ or ω do not significantly affect the pressure P.

According to Eq. (54), void growth rate is mainly affected by the threshold stress, P_∞, and less by the relative size of plastic zone, α. That is the case when growth rate is modest. Note that the threshold stress, P_∞, is directly related to yield stress via Eq. (51). In the situation of $P >> P_\infty$, however, the role of relative size of plastic zone, α, becomes more significant. At certain point, the higher yield stress leads to a smaller value of α so much so that the growth rate becomes higher. To make this point, Fig. 6(a) shows the macroscopic pressure, P, versus void growth rate, v, for the model material with two levels of yield stress: σ_Y = 100 MPa and 200 MPa. In the regime of low pressure (therefore low growth rate), material with higher yield stress grows slower for the same pressure. At a pressure P greater than a crossover of 12.16 GPa, the contrary is true (although hard

to read from the figure). That is, material with higher yield stress grows faster for the same pressure. By using Eq. (54), the crossover growth rate, v*, can be determined by

$$v^* = [\frac{P_{\infty 2} - P_{\infty 1}}{\frac{\rho}{2}(\alpha_1 + \kappa_1 - \alpha_2 - \kappa_2)}]^{\frac{1}{2}}. \tag{56}$$

In this expression, subscripts "1" and "2" denote the reference and comparison materials, respectively. Since the factor κ is a function of growth rate, Eq. (56) is solved numerically for specified material data. Results of crossover growth rate, v^*, and pressure, P^*, are shown in Fig. 6(b) using our model material as the reference material (σ_Y = 200 MPa); comparison material has yield stress ranging between 25 and 300 MPa. At a pressure $P < P^*$, (or $v < v^*$), growth rate is lower for materials with high yield stress. Conversely, at a pressure $P > P^*$, (or $v > v^*$), growth rate is higher for materials with high yield stress. Since Eq. (56) is fully symmetric with respect to reference and comparison materials, the roles of these materials can be swapped, yet crossover growth rate remains the same.

At this point, it calls for the remark that some of the calculations in the regime of high growth rate shown in Fig. 6(a) and (b) are questionable. According to Eq.(37), elastic zone is bounded between $r = D$ and $c_e t$. At a growth rate $v = c_e / \beta$, yield surface reaches the dilatational wave front. According to Eq. (39), $\kappa = 0$ for $v \geq c_e / \beta$. The limiting growth rate of c_e / β is shown in Fig. 6(b) for the considered range of yield strength. As shown, majority of the calculations fall beyond the limit. In order to better handle void growth at higher rate or high loading, the model has to include compressibility in plastic zone, and/or allow discontinuity due to shockwave (Hunter and Crozier, 1968). Since $\kappa = 0$ for $v \geq c_e / \beta$, it is interesting to observe that radial stress on yield surface, σ_D, is the same as that in quasistatic growth of Eq. (45).

4.2 Transient growth

In the following development, the approach of Section 2.3 is employed. The complete governing equation is obtained by Eq. (18) with σ_D from Eq. (44):

$$\frac{1}{3}\rho(\alpha+\kappa)R\frac{d^2R}{dt^2}+\frac{\rho(\alpha+\kappa)}{2}(\frac{dR}{dt})^2=P-\left(\frac{2}{3}\sigma_Y+\frac{2}{3}\sigma_Y\ln[(1-\frac{R_o^3}{R^3})\frac{2}{3\varepsilon_Y}]+\frac{2}{R}\gamma\right) \qquad (57)$$

This equation is solved numerically, because κ is a function of average growth rate too. Only brief applications of the model are given below, further discussion will be reported elsewhere.

According to Section 3, a critical stress σ_c is identified, which corresponds to the peak in the curve of stress versus void size (see Fig. 4). Theoretically, the critical stress approaches the threshold stress (or so-called cavitation limit stress) of Eq. (51) for infinite void size. Two loading levels are considered in the following calculations: subcritical ($P < \sigma_C$) and supercritical loading ($P > \sigma_C$). The critical stress is based on the initial void size, like that shown in Fig. 4. It needs to clarify that the work of Wu et al. (2003) also considers supercritical and subcritical loadings, but their critical stress is threshold stress (or cavitation limit stress) in our terminology.

For subcritical loading, void starts growing once the RHS of Eq. (57) becomes positive. It only grows to a limited size smaller than the critical size. As an example, for R_o = 5 nm, the critical stress σ_c is $5.834\sigma_Y$ and critical void radius $R_c = 1.325R_o$ = 6.625 nm. Fig. 7(a) shows the growth of the void subjected to a subcritical loading $P = 5.7\sigma_Y < 5.834\sigma_Y$. The growth rate increases at the moment load is applied; it reaches a maximum shortly, and starts declining to zero. The void ceases growing at R = 6.5 nm, which is less than the critical radius R_c of 6.625 nm.

Fig. 7(b) shows the results when a supercritical loading $P = 6\sigma_Y > 5.838\sigma_Y$ is applied. Void continues growing beyond the critical size which is 6.625 nm; and is expected to grow unbounded if the constant loading maintains unchanged. The grow rate is not monotonic though; it reaches a plateau before resumes increasing trend in the small time frame of 0.1 ns. The temporary reduction in growth rate is due to the growing resistance of elastic-plastic deformation (which is zero in the

beginning of growth). The critical condition is marked in Fig. 7(b), which indicates that largest resistance (relative sense) against void growth appears at critical condition. Fig. 8(a) shows growth rate on void of initial size $R_o = 5nm$ subjected to a range of macroscopic stress. As shown, macroscopic stress higher than $5.8\sigma_Y$ leads to unbounded growth whereas a stress of $5.7\sigma_Y$ does not. However, it is noticed that the stress of $5.8\sigma_Y$ is actually lower than the critical stress of $5.834\sigma_Y$ corresponding to $R_o = 5nm$. The reason unbounded growth is found at a stress of $5.8\sigma_Y < \sigma_c$ is that, in dynamic growth, void size may exceed the critical size corresponding to current void size before growth ceases. Growth rate for voids of a range of initial size is shown in Fig. 8(b). The loading P is slightly higher than the critical stress σ_c corresponding to void of $R_o = 5nm$, but sufficiently greater than those corresponding to $R_o = 7nm$ or higher so that the aforementioned plateau does not appear. For smaller void, the growth ceases shortly after expansion starts. The numerical results of Fig. 8 indicate that, for supercritical loading, void growth rate reaches a steady value at relatively large void size. This is discussed in previous section.

To gain a better understanding of the void growth process, energy components of Eqs. (5), (6), (8), and (15) for the plastic zone and Eqs. (36), (40) and (43) for elastic zone are calculated by using the solved growth rate; results are shown in the form of area chart in Fig. 9. Each of the components is normalized to the total energy supplied by the remotely applied pressure. Numerical results indicated the sum of calculated energy components by Eqs. (6), (8), and (15) is equal to the total energy of Eq. (5) for plastic zone; similarly for elastic zone. This confirms that the equations are solved properly. According to Eq. (8), kinetic energy in plastic zone has two components: $2\pi\rho\alpha R^2 v^3$ for inertia and $(4/3)\pi\rho\alpha R^3 v dv/dt$ for acceleration. As shown in Fig. 9(a) for a pressure slightly above the critical stress of $\sigma_c = 5.15GPa$ for void size $R_o = 10nm$, surface energy and kinetic energy for acceleration represent the major energy expenditure at the beginning. Energy in elastic zone is not negligible either. As void grows bigger, surface energy and, particularly, kinetic energy associated with acceleration drop quickly. At the same time, plastic dissipation and kinetic energy associated with inertia in plastic zone increase rapidly. Energy in elastic zone mainly spent on elastic strain energy which maintains constant proportion; kinetic energy represents a very small portion. As void becomes even bigger, energy expenditures are divided among plastic dissipation,

kinetic energy associated with inertia in plastic zone, and elastic strain energy. At higher loading, P, Fig. 9(b) shows higher proportion of kinetic energy associated with inertia in plastic zone, and elastic zone as well.

The proportion of energy expenditure in plastic and elastic zones maintains constant as void becomes bigger. According to Eq. (5), ratio of energy input to plastic zone to total energy provided by macroscopic stress P is σ_D / P. As void grows under constant macroscopic stress P, growth rate reaches a steady state value. The radial stress on yield surface, σ_D, becomes a constant, according to Eq. (44). This explains the observed constant proportion of energy in plastic and elastic zones. We can apply the similar treatment to all other energy components as well.

5. Concluding Remarks

A mathematical model is established to properly account for material compressibility and limited size of elastic deformation in dynamic growth of spherical void. It corrects the issue of excessive kinetic energy expenditure in elastic zone. A list of most significant remarks emerging from the study is:

1. The steady-state solution of radial stress on yield surface obtained by Hunter and Crozier (1968) does not reconcile with the solution assuming incompressibility. On the other hand, an approximate solution is developed, which can be used for general, transient growth.

2. A closed form of the stress-void size relation in quasistatic growth is obtained for the first time. It shows initial yielding on void surface takes place at $P = 2/3Y$ for large voids. For smaller voids of a few nanometers in size, macroscopic stress needs to overcome a critical stress for unbounded growth. Critical stress results from higher surface energy at decreasing void size. Based on the same reason, cavitation from void of zero size does not seem to be possible.

3. A crossover condition is identified pertaining to the effects of yield stress on void growth rate. At a growth rate/stress below the crossover condition, higher yield stress (i.e., work hardened) leads to lower growth rate. Reversal is true at growth rate/stress exceeding the crossover.

Acknowledgements

Support from the US Air Force SBIR Award (Contract No. FA8650-07-M-5232) with Dr. Patrick J. Golden, AFRL/MLLMN, Project Monitor, is gratefully acknowledged.

References

Ahn, D. C., Sofronis, P., Minich, R. J., 2006. On the micromechanics of void growth by prismatic dislocation loop emission. Mech. Phys. Solids 54, 735.

Ahn, D. C., Sofronis, P., Kumar, M., Belak, J., Minich, R. J., 2007. Void growth by dislocation-loop emission. Appl. Phys., 101, 063514.

Carroll, M. M., Holt, A. C., 1972. Static and dynamic pore-collapse relations for ductile porous materials. J. Appl. Phys. 43, 1626–1636.

Chung, D.T., Horgan, C. O., Abeyaratne, R., 1987. A note on a bifurcation problem in finite plasticity related to void nucleation. Int. J. Solids Structures 23, 983–988.

Cortes, R., 1992a. Dynamic growth of microvoids under combined hydrostatic and deviatoric stresses. Int. J. Solids Structures 29, 1637–1645.

Cortes, R., 1992b. The growth of microvoids under intense dynamic loading. Int. J. Solids Structures 29, 1339–1350.

Crozier, R. J. M, Hunter, S. C., 1970. Similarity solution for the rapid uniform expansion of a cylindrical cavity in a compressible elastic-plastic solid. Q. J. Mech. Appl. Math. 23, 349–363.

Gent, A. N., Tompkins, D. A., 1969. Surface energy effects for small holes or particles in elastomers. J. Polym. Sci. Part A2, 7, 1483.

Hill, R., 1989. The Mathematical Theory of Plasticity. Oxford science publications, Ox ford.

Huo, B., Zheng, Q. S., Huang, Y., 1999. A note on the effect of surface energy and void size to void growth, Eur. J. Mech. A/Solids 18, 987–994.

Huang, Y., Hutchinson, J. W., Tvergaard, V., 1991. Cavitation instabilities in elastic–plastic solids. J. Mech. Phys. Solids 39, 223–241.

Huang, M., Li, Z., Wang, C., 2007, Discrete dislocation dynamics modelling of microvoid growth and its intrinsic mechanism in single crystals, Acta Materialia 55, 1387-1396.

Johnson, J. N., 1981. Dynamic fracture and spallation in ductile solids. J. Appl. Phys. 52, 2812–2825.

Kameda, J., 1989. A microscopic model for the void growth behavior. Acta Metall. 37, 2067-2076.

Needleman, A. 1972. Void growth in an elastic-plastic medium. Journal of Applied Mechanics 39, 964-970.

Needleman, A., 1987. A continuum model for void nucleation by inclusion debonding. Journal of Applied Mechanics 54, 525-531.

Needleman, A., 1991. Strain rate effects on void nucleation by inclusion debonding, in *Mechanical Behavior of Materials - VI*, (ed. by M. Jono and T. Inoue), Vol. 3, Pergamon Press, Oxford, 151-156.

Nemat-Nasser, S., Hori, M., 1987. Void collapse and void growth in crystalline solids. J. Appl. Phys. 62, 2746–2757.

Ohashi, T., 2005, Crystal plasticity analysis of dislocation emission from micro voids, International Journal of Plasticity 21, 2071.

Ortiz, M., Molinari, A., 1992. Effect of strain hardening and rate sensitivity on the dynamic growth of a void in a plastic material. J. Appl. Mech. 59, 48–53.

Rice, J. R., Tracey, D. M., 1969. On the ductile enlargement of voids in triaxial stress fields. J Mech Phys Solids17, 201-217.

Rudd, R. E., Belak, J. F., 2002. Void nucleation and associated plasticity in dynamic fracture of polycrystalline copper: an atomistic simulation. Comp Mater Science 24, 148-153.

Seppala, E.T., Belak, J., Rudd, R. E., 2005. Effect of stress triaxiality on void growth in dynamic fracture of metals: A molecular dynamics study. Phys. Rev. B71, 064112.

Stevens, L., Davison, L., Warren, W. E., 1972. Spall fracture in aluminum monocrystals: a dislocation dynamics approach. J Appl. Phys. 42, 4922.

Tszeng, T.C., 2007a. Threshold condition of dislocation loop emission from microvoids. J. Appl. Phys. (submitted).

Tszeng, T.C., 2007b. Dynamic growth of cylindrical void by dislocation emission. Acta Materialia (submitted).

Tszeng, T.C., 2007c, Quasistatic and dynamic growth of cylindrical voids. J. Mech. Phys. Solids (to be submitted).

Tszeng, T.C., 2007d. A note on steady-state growth of spherical and cylindrical voids. J. Appl. Mech. (to be submitted).

Tvergaard, V., Huang, Y., Hutchinson, J.W., 1992. Cavitation instabilities in a power hardening elastic–plastic solid. Eur. J. Mech. A/Solids 11, 215–231.

Tvergaard, V., Hutchinson, J.W., 1993. Effects of initial void shape on the occurrence of cavitation instabilities in elastic–plastic solids. J. Appl. Mech. Trans. ASME 60, 807–812.

Tvergaard, V., Hutchinson, J. W., 2002, Two mechanisms of ductile fracture: void by void growth versus multiple void interaction. Int. J. Solids and Structures 39, 3581-3597.

Wang, Z. P., 1994. Growth of voids in porous ductile materials at high strain rate. J. Appl. Phys. 76, 1535–1542.

Warren, T. L., 1999. The effect of strain rate on the dynamic expansion of cylindrical cavities. J. Appl. Mech. 66, 818–821.

Wu, X. Y., Ramesh, K. T., Wright, T. W., 2003. The dynamic growth of a single void in a viscoplastic material under transient hydrostatic loading. J Mech. Phys. Solids 51, 1-26.

Figure(s)

Figures

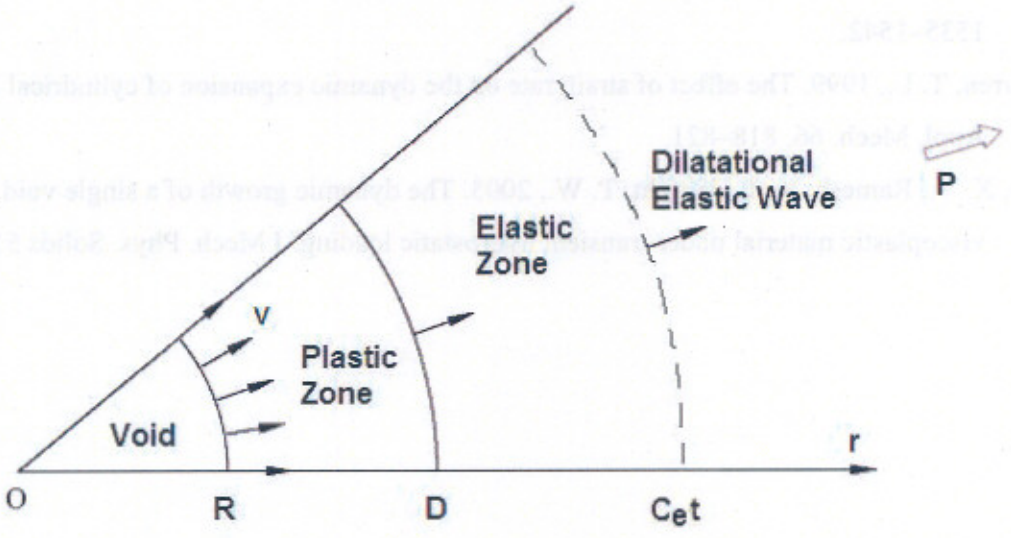

Fig. 1. Schematics of a expanding spherical void embedded in infinite matrix, subjected to remotely applied stress P. Void radius R, plastic zone radius D. Dilatational elastic wave propagates at speed c_e. Initial void radius is R_o.

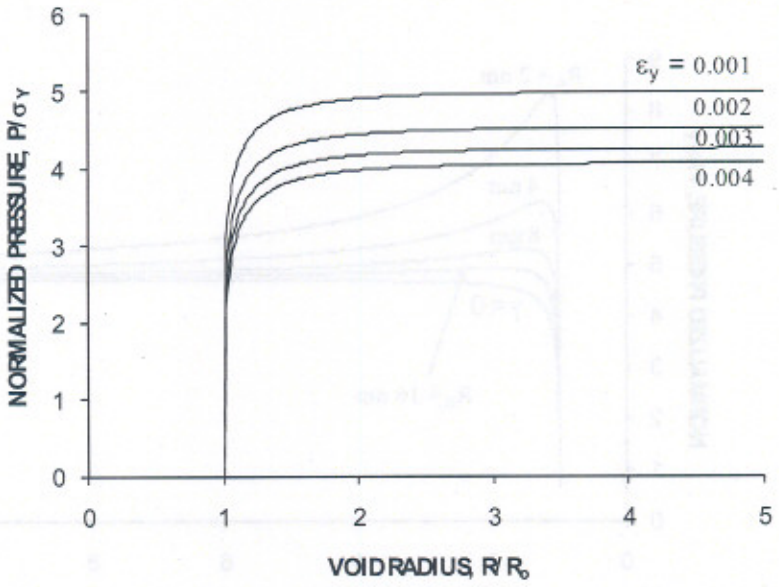

Fig. 2. Macroscopic pressure versus void size in quasistatic growth. $\varepsilon_y = \sigma_y / E$ is total strain at yielding. Surface energy density γ is zero.

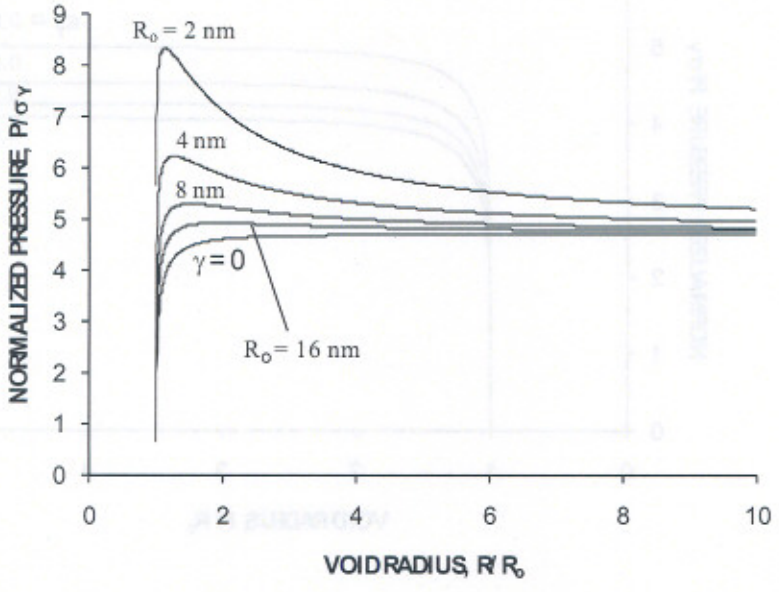

Fig. 3. Macroscopic pressure versus void size in quasistatic growth of void from a range of initial size, R_o. Surface energy density $\gamma = 1$.

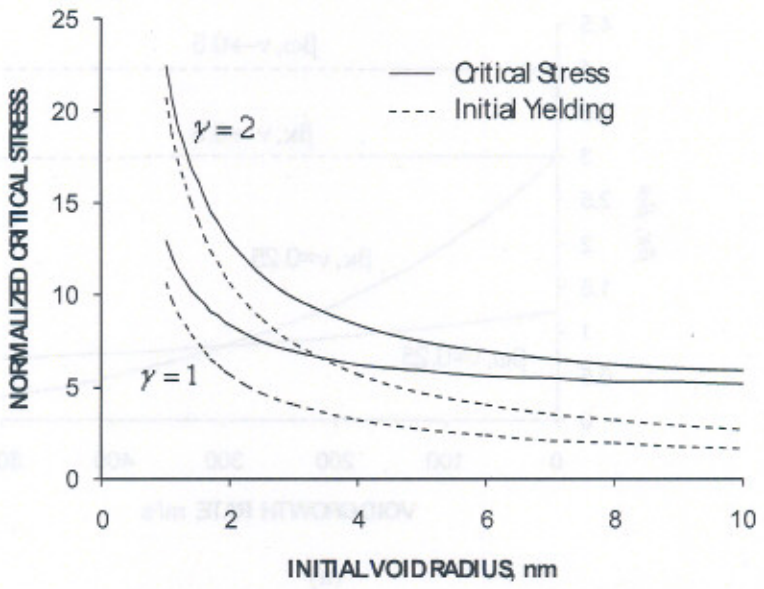

(a)

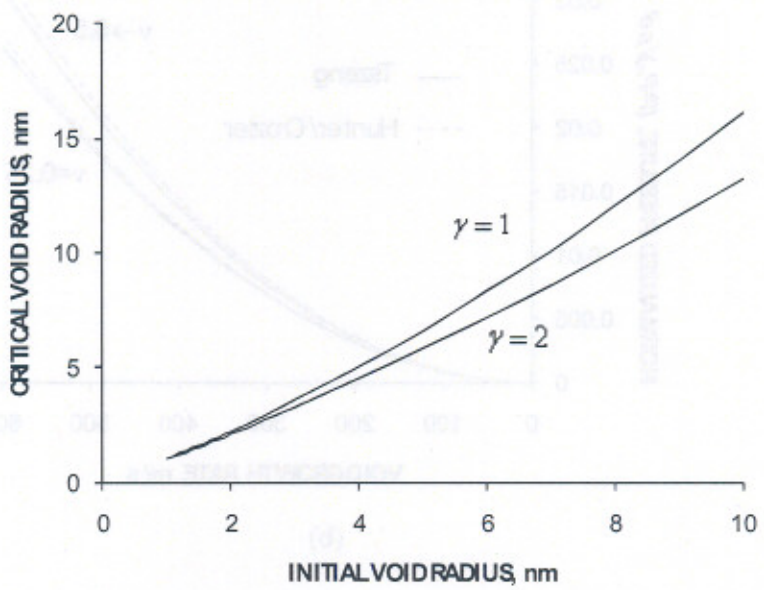

(b)

Fig. 4. (a) Critical stress, and (b) critical void radius for unbounded void growth as functions of initial void size. The critical stress is normalized by the yield strength, $\sigma_Y = 200MPa$ for the model material. Also shown in (a) are the pressure for initial yielding. Two levels of surface energy density are considered.

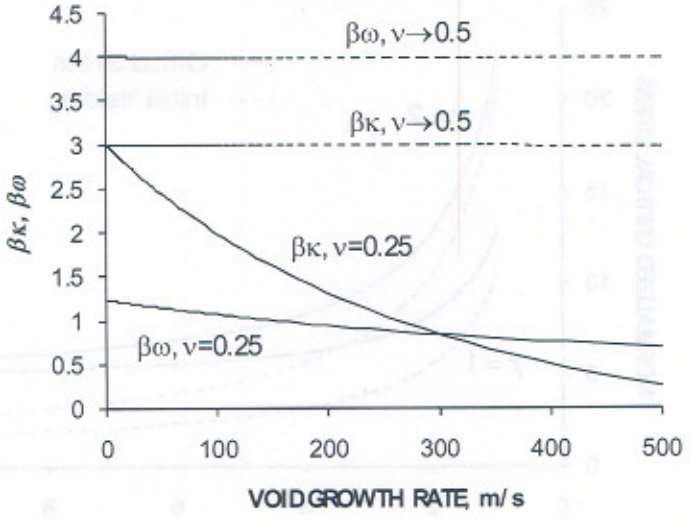

(a)

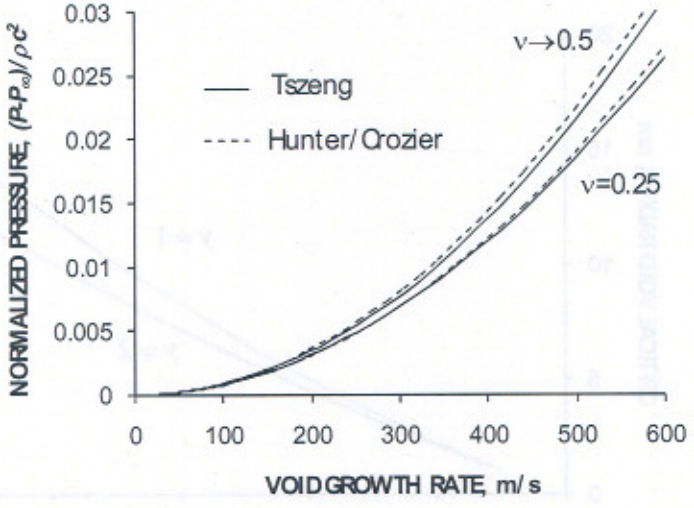

(b)

Fig. 5. (a) Factors κ and ω as functions of steady-state void growth rate; (b) Normalized pressure, $(P-P_\infty)/\rho c_e^2$, as function of steady-state growth rate, v. for model of Section 2.2 (Hunter/Crozier) and Section 2.3 (Tszeng). Property data are taken from model material, except two indicated values of Poisson's ratio are used. $\nu = 0.499999$ for near-incompressible material.

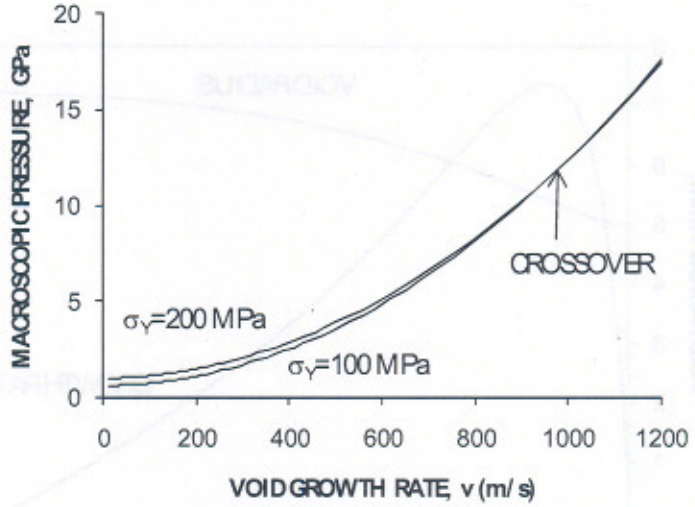

(a)

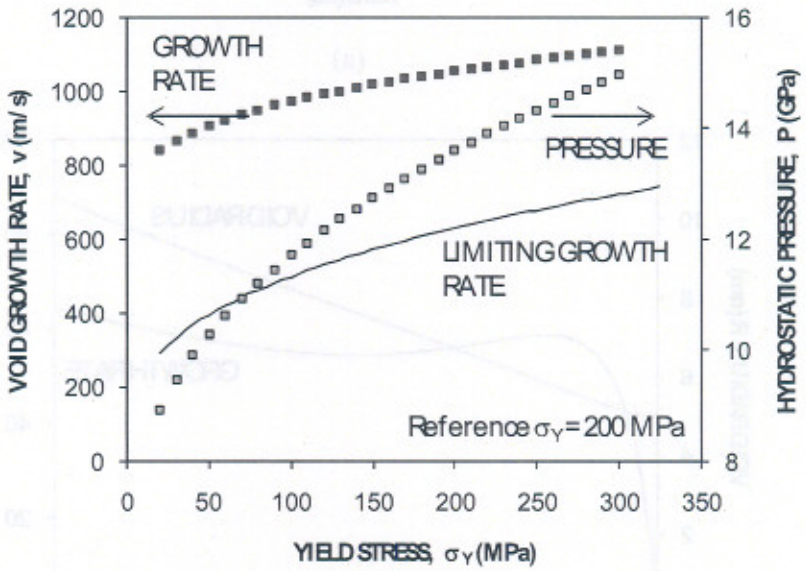

(b)

Fig. 6. (a) Pressure, P, as function of steady-state growth rate, v. for model materials but two values of Young's modulus as indicated. Crossover is found at v*= 1,000.16 m/s and P*= 12.16 GPa. (b) Crossover growth rate, v*, and pressure, P*, as function of yield stress, σ_Y. Model material (σ_Y = 200 MPa) is used as reference. Limiting growth rate corresponding to $\kappa = 0$ (zero elastic zone) is also shown.

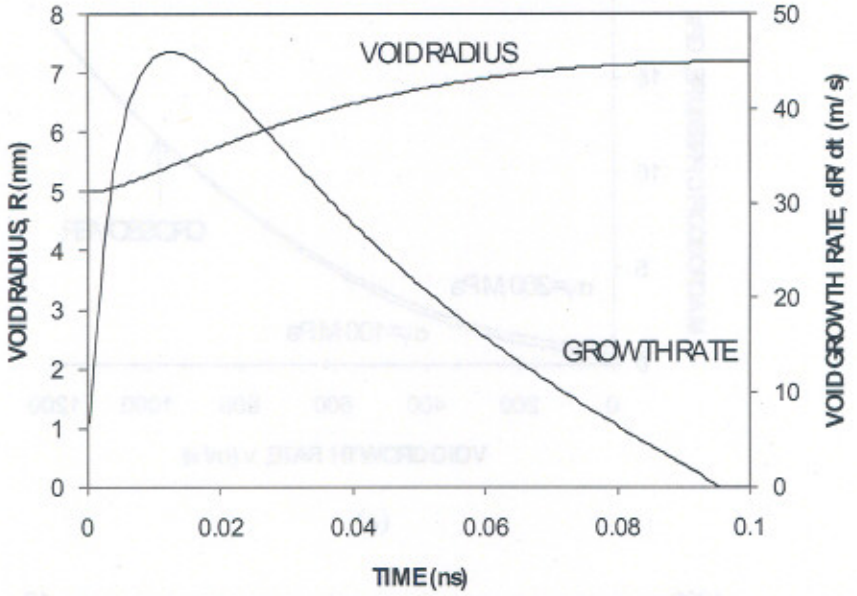

(a)

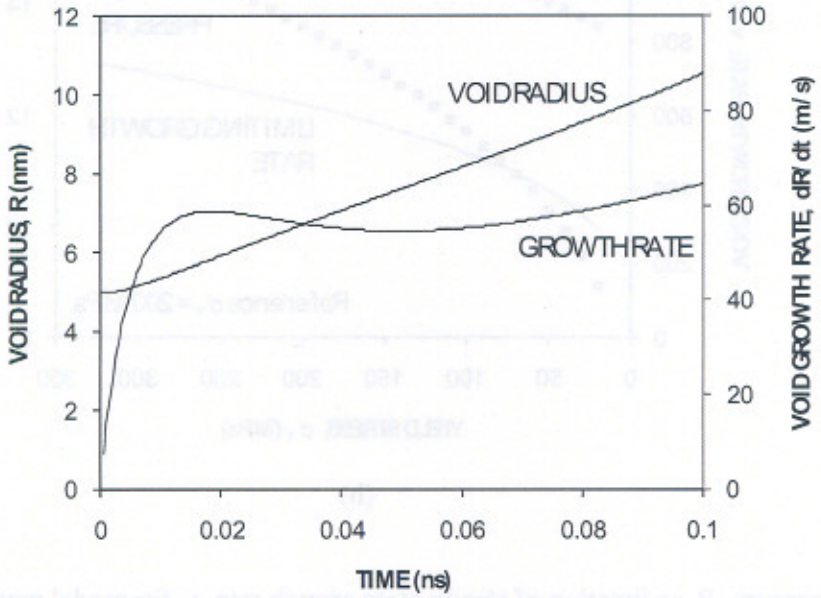

(b)

Fig. 7. Dynamic growth of void. (a) Subcritical loading, $P = 5.7\sigma_Y < 5.834\sigma_Y$. (b) Supercritical loading, $P = 6\sigma_Y > 5.834\sigma_Y$. Initial void radius $R_o = 5$ nm. Property data from model material.

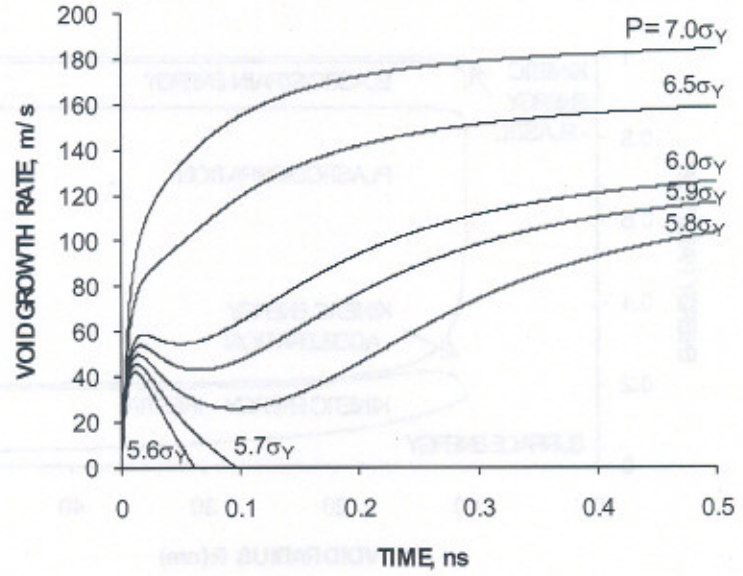

(a)

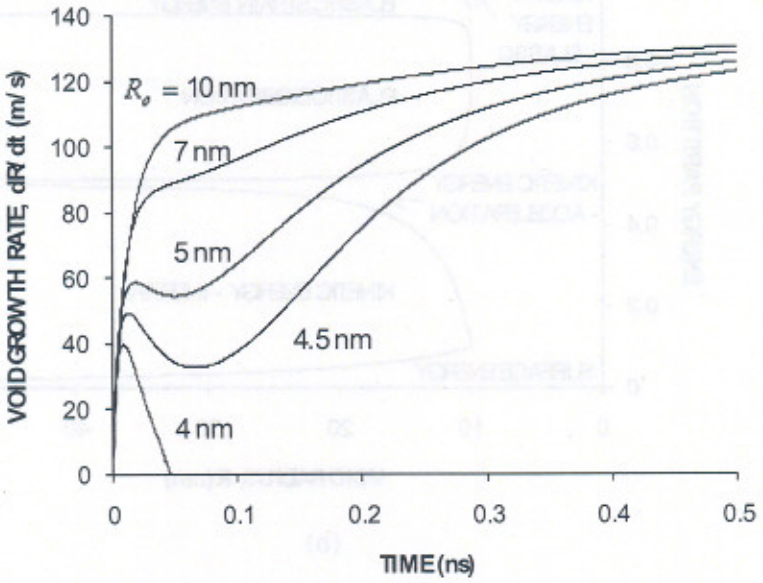

Fig. 8. Growth rate in subcritical and supercritical loading. (a) Loading stress is below and above the critical stress of $\sigma_c = 5.834\sigma_Y$. Initial void size $R_o = 5nm$; (b) Growth from void of a range of initial size. $P = 6\sigma_Y > 5.834\sigma_Y$.

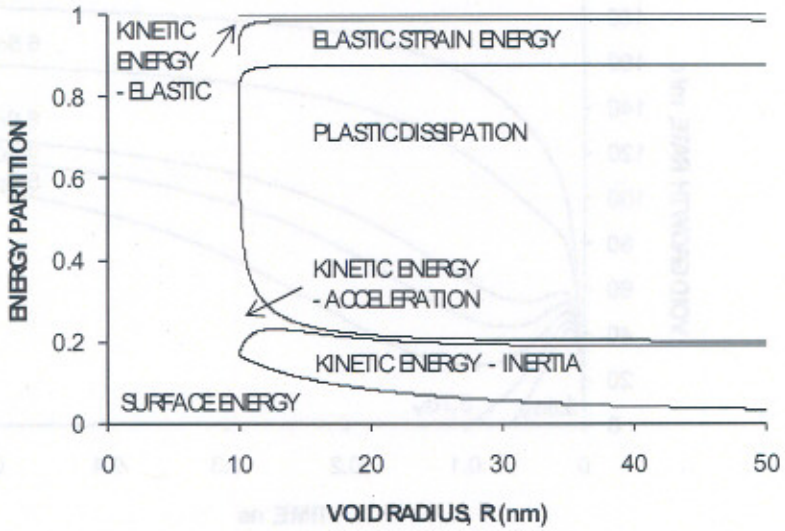

(a)

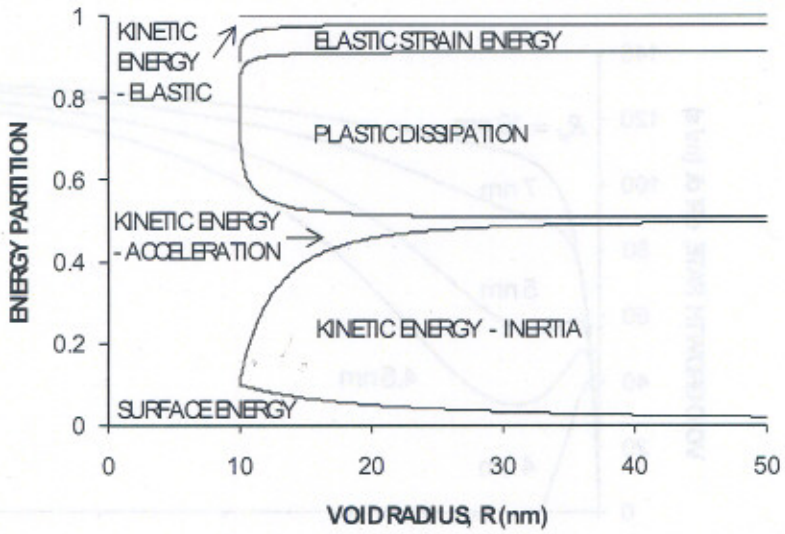

(b)

Fig. 9. Area chart of energy expenditure in the process of supercritical void growth. All energy components are normalized to the total energy supplied by the externally applied pressure. Initial void size $R_o = 10$ nm. (a) $P = 6\sigma_Y$, (b) $P = 10\sigma_Y$.